Accepted Manuscript

Submission Date: 2024-01-20
Accepted Date: 2024-03-26
Accepted Manuscript online: 2024-04-03

Experimental and Clinical Endocrinology & Diabetes

Beneficial effects of Echinacoside on cognitive impairment and diabetes in type 2 diabetic db/db mice

Fanglin Qin, Yiming Yan, Ningxi Yang, Yarong Hao.

Affiliations below.

DOI: 10.1055/a-2298-4593

Please cite this article as: Qin F, Yan Y, Yang N et al. Beneficial effects of Echinacoside on cognitive impairment and diabetes in type 2 diabetic db/db mice. Experimental and Clinical Endocrinology & Diabetes 2024. doi: 10.1055/a-2298-4593

Conflict of Interest: The authors declare that they have no conflict of interest.

This study was supported by Hubei Natural Science Foundation of China, No.2016CFB673

Abstract:
Cognitive dysfunction is an important comorbidity of diabetes. Insulin resistance may play a critical role in diabetes-related cognitive impairment. Echinacoside(ECH), a natural phenylethanoid glycoside, is the active component of anti-diabetes prescriptions in traditional Chinese medicine. Its effect on modulating insulin resistance has been confirmed but modulating neurodegenerative disease still remains to be clarified. Db/db mice, a spontaneous Type 2 diabetes （T2D）mode, were intragastrically administered various doses of ECH or an equivalent volume of saline. Weight, blood glucose, and insulin resistance index were measured. Morris water maze was used to observe the compound effects on cognition. Hippocampal lesions were observed by histochemical analysis. In db/db mice, ECH alleviates diabetes symptoms, memory loss, and hippocampal neuronal damage.Following the step, we found CD44 and phosphorylated tau expression upregulated in diabetic mice. We also found the insulin receptor substrate-1 (IRS1)/phosphatidylinositol 3-kinase (PI3K)/protein kinase B (AKT) signaling pathway dysregulated in diabetic mice. All these changes could be reversed by ECH. Our study provides theoretical support and experimental evidence for the future application of ECH in diabetic cognition dysfunction treatment, promoting the development of traditional medicines.

Corresponding Author:
Prof. Yarong Hao, Renmin Hospital of Wuhan University, Wuhan, China, hyrtg2023@163.com

Affiliations:
Fanglin Qin, Renmin Hospital of Wuhan University, wuhan, China
Yiming Yan, Renmin Hospital of Wuhan University, Wuhan, China
Ningxi Yang, Renmin Hospital of Wuhan University, Wuhan, China
Yarong Hao, Renmin Hospital of Wuhan University, Wuhan, China

This article is protected by copyright. All rights reserved.

Accepted Manuscript

This is a PDF file of an unedited manuscript that has been accepted for publication. As a service to our customers we are providing this early version of the manuscript. The manuscript will undergo copyediting, typesetting, and review of the resulting proof before it is published in its final form. Please note that during the production process errors may be discovered which could affect the content, and all legal disclaimers that apply to the journal pertain.

Thieme

Beneficial effects of Echinacoside on cognitive impairment and diabetes in type 2 diabetic db/db mice

Fanglin Qin [1], Yiming Yan[1], Ningxi Yang[1], Yarong Hao[1]*

Department of Geriatrics, Renmin Hospital of Wuhan University, 99 Zhang Zhidong Road, Wuchang District, Wuhan, Hubei Province 430060, China
Email:
Yiming Yan[1]
Department of Geriatrics, Renmin Hospital of Wuhan University, 99 Zhang Zhidong Road, Wuchang District, Wuhan, Hubei Province 430060, China
Email:
Ningxi Yang[1]
Department of Geriatrics, Renmin Hospital of Wuhan University, 99 Zhang Zhidong Road, Wuchang District, Wuhan, Hubei Province 430060, China
Email:
[*] **Correspondence author:**
Yarong Hao[1*] Ph.D
[1*] Department of Geriatrics, Renmin Hospital of Wuhan University, 99 Zhang Zhidong Road, Wuchang District, Wuhan, Hubei Province 430060, China.
Email:
Tel:+8618771035142
Business Telephone: 02788041911+86374
There is no conflict of interest among the authors.

Abstract

Cognitive dysfunction is an important comorbidity of diabetes. Insulin resistance may play a critical role in diabetes-related cognitive impairment. Echinacoside(ECH), a natural phenylethanoid glycoside, is the active component of anti-diabetes prescriptions in traditional Chinese medicine. Its effect on modulating insulin resistance has been confirmed but modulating neurodegenerative disease still remains to be clarified. Db/db mice, a spontaneous Type 2 diabetes （T2D）mode, were intragastrically administered ECH by or an equivalent volume of saline. Weight, blood glucose, and insulin resistance index were measured. Morris water maze was used to observe the compound effects on cognition. Hippocampal lesions were observed by histochemical analysis. In db/db mice, ECH alleviates diabetes symptoms, memory loss, and hippocampal neuronal damage.Following the step, we found CD44 and phosphorylated tau expression upregulated in diabetic mice. We also found the insulin receptor substrate-1 (IRS1)/phosphatidylinositol 3-kinase (PI3K)/protein kinase B (AKT) signaling pathway dysregulated in diabetic mice. All these changes could be reversed by ECH. Our study provides theoretical support and

This article is protected by copyright. All rights reserved.
Accepted Manuscript

experimental evidence for the future application of ECH in diabetic cognition dysfunction treatment, promoting the development of traditional medicines.

Keywords

Echinacoside; diabetes; cognitive impairment; insulin resistance.

1. Introduction

As a global public health issue, diabetes adversely affected more than 500 million people with multiple chronic complications worldwide[1]. Particularly, the cognitive dysfunction is one of the most serious complications, which is intricately correlated with the type 2 diabetes (T2D), more than 90% of diabetes patients[2]. Approximately 50% T2D encountered cognitive decline, including the structural and functional brain impairment, with more gray matter atrophy, faster brain aging speed, worse control of memory and information-processing[3-5].

T2D-related cognitive diseases include the asymptomatic cognitive decline, the mild cognitive impairment (MCI) and dementia. The vascular dementia (VaD) and Alzheimer's disease(AD) are most common types among these[6, 7]. It was suggested that aincidence of AD in cases with preexisting diabetes is nearly 1.5 times than others [8, 9]. Considering the correlation between AD and diabetes, researchers even pointed that AD could be referred to as "brain diabetes" or "type 3 diabetes" [10, 11]. However, the diabetes-specific drugs cannot slow or decrease slow cognitive dysfunction, although previous studies showed that metformin might reduce cognitive decline[7, 12]. Overall, despite the prevalence and harmfulness of diabetic encephalopathy, more effective cures for diabetes-related cognitive dysfunction still remain to be continuously explored [13].

According to clinical trials and experiments in vitro and in vivo, natural products from plants are promising for prevention and management of T2D-related complications [14-17]. Cistanche tubulosa, the most commonly used tonic Chinese medicine, might alleviate Alzheimer's disease and cerebral ischemic injuries [18-20]. Moreover, consistent with our previous finding[21], researchers suggested that cistanche tubulosa showed beneficial effects on diabetes and diabetic complications in mouse models[22-24].

Identifying the potentially effective components from natural herbs might provide sources for new drugs development for diabetic encephalopathy therapy[25-27]. Echinacoside(ECH) is the most active component of Cistanche tubulosa. Previous studies showed ECH might be promising for treatment in depressive disorders, vascular dementia, cerebral ischemia, Parkinson's disease, and Alzheimer's disease[28-31] [32]. For mechanisms, ECH freely crosses the blood-brain barrier, showed effects of neuroprotection, anti-oxidative stress, anti-neuroinflammation,

This article is protected by copyright. All rights reserved.
Accepted Manuscript

regulation of apoptosis and autophagy [33]. However, effects of ECH on type 2 diabetes-related cognitive dysfunction are still limited.

Hyperphosphorylation tau(p-tau) aggregation in neurofibrillary tangles (NFTs) is closely associated with cognitive decline in neurodegeneration disease[34, 35].A lot of studies pointed out that p-tau has a tight link with (GSK3β)[36, 37]. PI3K/AKT/GSK3β is a classical pathway activated by insulin. Under physiological conditions, active AKT inhibits GSK3β to modulate the phosphorylation balance of tau[36]. Thus, p-tau comes out when insulin resistance happens[38, 39]. Bioinformatics analysis shows CD44, a biomarker of astrocyte cells, is positively correlated with T2D and AD through inflammation and insulin resistance[40]. Soluble CD44 secreted from glioblastoma cells induces neuronal degeneration through the activation of tau pathology in the brain[41]. The level of CD44 expression in the brain of db/db mice and its relationship with insulin resistance has not been reported well. Our study tries to explore whether ECH has an effect on improving cognitive impairment in db/db mice, and the effect on insulin resistance, p-tau, and CD44.

Herein, in this study, we focused on the potentially beneficial regulation of ECH on cognitive impairment in db/db mice, one representative mice model of type-2 diabetes. Besides, for a better understanding of the behind mechanisms, we evaluated the effects of ECH on insulin resistance, hyperphosphorylation tau(p-tau) aggregation, and CD44, three important markers or events highly correlated to type 2 diabetes and neurodegeneration diseas[38-40].

2. Method

2.1. Experimental Animals

The Institutional Animal Care and Use Committee(IACUC) of Renmin Hospital of Wuhan University granted approval for the experimental procedures (Issue number:20190517). Our animal care and handling practices strictly adhered to the declaration of Helsinki and the guidelines set forth by Renmin Hospital, Wuhan University. We obtained eight-week-old male C57BLKS/J db/db mice and db/m mice (SPF grade) from Nanjing University, specifically from the Nanjing Institute of Biomedicine in China.

2.2. Main instruments and reagents

The Shanghai Medical Science Company (ECH No.190906, China) dissolved ECH in water at a concentration of 2 mg/mL. Afterwards, the solution was stored at a temperature of 4℃ in a dark environment. Insulin ELISA kit(abcamab,277390), Hematoxylin and Eosin Staining Kit instructions (Beyotime, C0105S), Nissle Staining Kit instruction (Solarbio,G1436), BCA protein concentration detection kit (Beyotime,P0010). SDS-PAGE gel preparation kit (Epizyme,PG112), TRIzol reagent(Thermofisher,15596026), One-step gDNA Remover (Servicebio,G3337), SYBR Green Supermix (Servicebio,G3326), BeyoECL Plus(Beyotime, P0018M).

2.3. Animal grouping and treatment

This article is protected by copyright. All rights reserved.

Accepted Manuscript

To conduct the experiment, a group of mice aged 10 weeks was isolated for 1 week and provided with adaptive feeding for an additional week. Then, the mice were divided randomly into three groups: control group (db/m, n=7), diabetic model group (db/db, n=7), and ECH treated group (db/db+ECH, n=7). At 12 weeks, the normal control group and mice in the diabetic model group were both given normal saline (0.05 mL/10 g) via intragastric administration. However, the ECH-treated group of mice received a daily dose of 300 mg/kg of ECH, which was administered through intragastric administration[21]. Throughout the 14-week experimental period, the mice had unrestricted access to food and water. After the 14-week intervention, The mice were anesthetized by intraperitoneal injection of 2% pentobarbital sodium (100mg/kg) in order to collect blood samples. The serum was then separated and immediately stored at −80°C for further analysis after inserting a capillary needle. To eliminate blood residue, brain perfusion was performed with PBS, and any excess PBS was removed using filter paper. The brains hippocampus were then obtained and subjected to examination using histology, western blot, and RT-PCR methods.

2.4 General condition

Every two weeks, the mice were carefully weighed and their blood glucose levels were accurately measured. Upon reaching the end of week 26, following an 8-hour fasting period, blood samples were collected from the mice through punctures made on their tail veins. The Fasting Plasma Glucose (FPG) levels were then measured using a highly reliable blood glucose meter(Johnson & Johnson, New Brunswick, NJ, USA). While performing the OGTT experiment, mice was performed by gavage of glucose 2g/kg. The blood glucose values of mice were measured at 0 min before glucose loading, 15, 30, 60 and 120 min after glucose loading, and the area under the curve of time blood glucose value was calculated. Fasting insulin levels (FINS) were measured by utilizing the ELISA kit (abcamab,277390) according to the manufacturer's instructions. A standard curve was constructed using the concentration and optical density (OD) values of the standard sample, enabling the calculation of the sample concentration. The insulin resistance index (HOMA-IR) was calculated using the following formula: HOMA-IR = FPG × FINS/22.5.

2.5. Morris Water Maze

Morris's water maze test was used to measure spatial learning and memory in mice after 16 weeks of intervention. Water maze apparatus includes circular polypropylene pool with four different patterns surrounding it to aid mice in navigating. Non-toxic white milk was added to the water to make it opaque, and the pool was filled with water maintained at 23 ± 1 °C. To acclimatize the mice to their new environment, they were given a two-minute free-swim session before the test. During 5 consecutive days, the mice were given 4 trials each, with a 15-minute inter-trial interval. During the trial, the maximum trial time was 60 seconds, and subjects were manually guided if they did not reach the platform within that time. Following the 5 days of task acquisition, a probe trial was presented. During the probe trial, the platform was removed, and each mouse was placed in the water (head facing toward the wall) from

This article is protected by copyright. All rights reserved.
Accepted Manuscript

the quadrant opposite the quadrant where the platform was original. The platform was removed during the probe trial. Mice were placed in the opposite quadrant of where the platform, but head toward wall. Additionally, we recorded the time spent in the platform and target quadrant, the target platform crossings, and the mean speed of the target quadrant within the 60s.

2.6. HE/Nissl staining

We fixed the perfused brain tissues in 4% PFA solution for 24 hours after collection. Then, the brain tissues were dehydrated in alcohol, embedded in paraffin wax, and cut into 5 μm thick sections from the coronal plane. Dewaxed brain sections were then rehydrated, dyed, dehydrated, and transparent according to the Hematoxylin and Eosin Staining Kit instructions (Beyotime, C0105S) and Nissle Staining Kit instructions (Solarbio, G1436). Finally, we observed the slides under a light microscope (Olympus, Japan).

2.7. Bioinformatics analysis

In order to navigate the expression level of CD44 in disease and normal tissues, two datasets were involved in this study (GSE122063 and GSE161355), both from the GEO database (https://www.ncbi.nlm.nih.gov/geo/). The GSE122063 datasets were in the GPL16699 platform including 8 VAD,12 AD, and 11 controls brain tissue for future analysis[42]. The GSE161355 datasets were in the GPL570 platform including 6 T2D and 5 control brain tissue[43]. The probe identification numbers were converted into the official gene symbols according to the GPL16699 and GPL570 platforms. After log2 transformation and normalization, the “LIMMA” package[44] built-in R software(version 4.3.1) was used to identify the differentially expressed genes(DEGs). The cutoffs were $P<0.05$ and false discovery rate (FDR) < 0.05. The average expression was taken when multiple probes corresponded to one. In the procession, we uploaded these genes to Hiplot drawing Wayne's diagram. Then, extract CD44 expression from geneMatrix files to analyze the differentially expressed level in the two datasets. Next, we evaluated enriched biological processes (BPs), molecular functions (MFs), and cellular components (CCs) using the "GO plot" package. PvalueCutoff = 0.05 and qvalueCutoff =0.05 were set as the thresholds for enrichment analysis. Then we uploaded target genes into the STRING database to predict the PPI network.

2.8. qRT-PCR Analysis

Total RNA was extracted from the frozen brain using TRIzol reagent(Thermofisher, 15596026), and was reverse-transcribed to cDNA and amplified with a commercial One-step gDNA Remover (Servicebio, G3337). qRT-PCR analysis was conducted on a Bio-Rad CFX Connect real-time PCR system (Bio-Rad, CA, USA) with cDNA, forward and reverse primers, and SYBR Green Supermix (Servicebio, G3326). Internal control was GAPDH, which was used to calculate the relative expression level of mRNA . Gene-specific primers were as follows: CD44, F:5’-TGGCTCATCATCTTGGCATCT-3’ and R: 5’-TCCTGTCTTCCACCGTCCC-3’;

This article is protected by copyright. All rights reserved.
Accepted Manuscript

GAPDH, F:5'-CCTCGTCCCGTAGACAAAATG-3' and R: 5'-TGAGGTCAATGAAGGGGTCGT-3'.

2.9. Western Blot Analysis

After treatment with specific experimental conditions, the total proteins of hippocampus tissue were isolated by RIPA lysis buffer(Servicebio,G2002) with a protease inhibitor(Servicebio,G2006), phosphatase inhibitor(Servicebio ,G2007), and 0.1 M PMSF (Beyotime, ST507). Using Liquid Nitrogen Grinder and Ultrasonic Grinding to cleavage the tissues. We then collected the supernatants and used the BCA reagent (Beyotime, P0010) to determine the protein content. Following the electrophoresis, equal amounts of protein were separated on 10% sodium dodecyl sulfate-polyacrylamide gels and transferred onto polyvinylidene difluoride membranes. After being blocked by 5% nonfat milk, the membranes were incubated with different primary antibodies: IRS-1(CST,#2382,1:1000), phospho-IRS-1(Ser307) (ABclonal, AP0552, 1:800), PI3K(p110)(ABclonal, A22730, 1:800), CD44(CST,#3570,1:1000), phospho-AKT (S473) (CST, #4060,1:1000), AKT(CST,#9272,1:1000), GSK3β(Wanleibio, WL10456,1:500), and phospho-GSK3β(CST,#5558,1:1000), tau(Proteintech,10274-1-AP,1;2000), phospho-tau(Proteintech,82568-1-RR1 : 2000) at 4 °C for 12h~18h. At room temperature, membranes were incubated for 1 hour with the secondary antibodies: Anti-Mouse (Proteintech, SA00001-1,1 : 5000), Anti-Rabbit (Proteintech,SA00001-2,1 : 5000).GAPDH (ABclonal,AC002,1:5000)was used as an internal control. The immunocomplexes were finally observed with a UVP BioSpectrum 415 Imaging System (Upland, CA, USA).

2.10. Statistics analysis

Western Blot experimental bands were analyzed by Image J software for gray value, SPSS 26.0 software for statistical analysis of data and GraphPad Prism 8.0 for plotting. One way ANOVA (one way ANOVA) was used to compare the differences of the data, SNK-q test was used for further two-by-two comparisons, combined with the LSD test to compare the differences between groups, and the results of the measurement data conforming to the normal distribution were expressed as the mean plus or minus the standard error of the mean (Mean±SEM), and the difference of $P<0.05$ was considered to be statistically significant.

3. Results

3.1. Cross analysis of the molecular links between type 2 diabetes and Alzheimer's diseas

Previous studies uncovered genes and signatures crosstalk linked these two diseases[45-48]. Herein, differentially expressed genes (DEGs) between AD and control including 381 downregulated genes and 357 upregulated genes in the dataset GSE122063**(Fig.1.A)**. DEGs between T2D and control including 95 downregulated genes and 256 upregulated genes in the dataset GSE161355**(Fig.1.A)**. The common

This article is protected by copyright. All rights reserved.

Accepted Manuscript

upregulated genes include SERPINA3, GEM, MAFF, DNAJB1, SPP1, HSPB1, GFAP, CD44. The common downregulated genes include ADHFE1 and BDKRB1. Enrichment analysis showed that the functions of most DEGs enriched in cell projection, extracellular exosome, and inflammatory response metascape ect**(Fig.1.C)**. Among these DEGs, particularly, CD44 was tightly correlated with diabetes, insulin resistence and inflammatory response[40, 49] **(Fig.1.D)**. Herein, we verified that CD44 was upregulated in both two datasets with $P<0.05$. Particularly, we found a significant difference in the CD44 expression between the control group and the disease group in the two datasets**(Fig.1.B)**. In the GSE122063, the *P* value of CD44 expression was less than 0.001, in the temporal or frontal cortex between AD and control group. In the GSE161355, the *P* value of CD44 expression was less than 0.05, in the temporal cortex between T2D and control group**(Fig.1.B)**. In the GO enrichment analysis of the common DEGs between AD and T2D, CD44 was involved in cell projection, extracellular exosome, inflammatory response, and protein binding**(Table 1)**.

3.2. ECH alleviated disorders of general health condition and insulin resistance in diabetic mice

Changes in body weight and fasting plasma glucose of three groups were detected fortnightly. For the weight gain, both the db/db+ECH and db/db groups increased significantly greater than the db/m group at the beginning of diet treatment, and kept significantly different during the remaining weeks **(Figure 2A)**. However, compared with the db/db group, there was a relatively lower body weight gain in the db/db+ECH group. For the glucose level, the fasting plasma glucose level (FPG) of db/db mice increased significantly and fluctuated dramatically compared with the db/m group **(Figure 2B)**. Besides, ECH intervention decreased the level and fluctuation of FPG compared to the db/db group. Following OGTT, the db/db group experienced a significant delay in glucose clearance**(Figure 2D)**. The AUC was significantly higher in db/db **(Figure 2E)**. More importantly, ECH intervention significantly reduced AUC, and improves glucose clearance in db/db mice**(Figure 2D-2E).**

To clarify the effects of ECH on insulin sensitivity, we further evaluated the level of insulin and HOMA-IR in each group at the end of the test. Insulin content in the db/db mice (22.09 ± 1.26 mIU/L) was distinctly higher than that of the control group (6.57 ± 0.51 mIU/L) and ECH intervention significantly decreased insulin levels **(Figure 2C)**. HOMA-IR is another one reliable indicator to evaluate insulin resistance. HOMA-IR(HOMA-IR = FPG × FINS/22.5) was significantly enhanced in the db/db group compared with the db/m group **(Figure 2F)**, which indicated serious insulin resistance. After ECH intervention, HOMA-IR was notably diminished compared to that of the db/db group **(Figure 2F)**.

3.3. ECH partially restore the cognitive impairment in diabetic mice

This article is protected by copyright. All rights reserved.
Accepted Manuscript

Morris water maze (MWM), as a widely used behavioral experiment reflecting cognitive ability, was selected to examine the spatial learning and memory ability of mice. The escape latency of the db/db group kept significantly longer than the db/m group and db/db-ECH group during five days of training **(Figure 3A)**. Overall, the escape latency on day5 of db/db-ECH (21.60±1.89) group is significantly lower than db/db group (38.73±4.52), which indicated ECH improved the cognitive function of T2DM mice **(Figure 3B)**. Similarly, compared with the db/m group, the db/db group showed cognitive impairment, with a significantly lower value of target platform crossings, a slower mean speed of the target quadrant in the probe trial, a shorter time spent in the platform and target quadrant **(Figure 3C-3E)**. After the ECH intervention, the platform crossing **(Figure 3C)**, mean speed of target quadrant**(Figure 3D)**, and the platform quadrants **(Figure 3E)** significantly increased. The swimming track of the db/db group tended to be marginal, but showed a more activity way of exploring in db/db-ECH group**(Figure 3F)**.These data indicated that ECH partially restored the learning and memory impairment of diabetic mice.

3.4. ECH ameliorates the histomorphologic damage of the hippocampus in diabetic mice

For exploring the effects of ECH on brain damage, the cell arrangement and number of neurons in the hippocampus of diabetic mice were evaluated through HE and Nissl staining. The hippocampal regions in the db/m group presented regular cell arrangement in HE staining. In the db/db group, disorder arrangement, and nuclei pyknosis of neurons were observed in DG, CA3, and CA1 regions **(Figure.4A)**. After ECH was gavaged, these damages were alleviated **(Figure 4A)**. The number of neurons in the control and treatment groups are shown by Nissl staining**(Figure 4B)**. In the db/db group, the number in the DG and CA3 regions was remarkably reduced compared with the db/m group **(Figure 4C)**. After being gavaged with ECH, the number of surviving neurons in hippocampal DG and CA3 areas of the ECH group was notably enhanced **(Figure 4B)**. These results displayed that ECH prevented the loss of neurons in the hippocampus of diabetic mice.

3.5. ECH reduced the mRNA and protein expression of CD44 in diabetic mice

In order to verify the upregulated expression of CD44 in T2DM and potential link to ECH, the expression levels of mRNA and protein in the db/db mice were evaluated by qRT-PCR and western blot. As shown in **Fig.5**, the mRNA expression and protein levels of CD44 in the db/db group were remarkably decreased compared with the db/m group ($p < 0.01$). However, the treatment with ECH caused remarkable restoration of the mRNA and protein expressions in contrast with the db/m group.

3.6 ECH affected the phosphorylation of IRS-1/PI3K/AKT/GSK-3β and tau in diabetic mice

Hyperphosphorylation tau(p-tau) aggregation in neurofibrillary tangles (NFTs) is closely associated with cognitive decline in neurodegeneration disease[34, 35]. The balance of p-tau/tau is regulated by GSK3β, which is negatived by phosphorylation at the site of ser9[36]. Western blot was used to determine the expression of GSK-3β□p-

This article is protected by copyright. All rights reserved.
Accepted Manuscript

GSK-3β(Ser9)tau and p-tau(S202/T205) protein among different groups. As shown in **Fig.6A-B**, there was no significant difference was found among the three groups in the protein expression of GSK3β and tau. However, a variation was found in the content of phosphorylation protein. As shown in **Fig.6A-B**, the ratio of p-GSK-3β(Ser9)/GSK-3β in the diabetic group was lower than that of the db/m group (p<0.05), but the ratio of p-tau(S202/T205)/tau protein was higher. However, administration with ECH enhanced the ratio of p-GSK-3β(Ser9)/GSK-3β and decreased the ratio of p-tau(S202/T205)/tau compared to the diabetic group(p<0.05). Less tau phosphorylation means reduced pathological alterations. ECH decreased relative p-tau(S202/T205) level indicated its effect on rescuing detrimental changes in the diabetic brain.

Gsk3β was mainly regulated by the IRS-1/PI3K/AKT insulin signaling pathway[36, 38]. In order to investigate the molecular mechanism of ECH on the phosphorylation of GSK-3β, the western blot was used to evaluate the expression levels of IRS-1/PI3K/AKT pathway protein in the three groups. As shown in **Fig.6C-D**, the protein expression levels of IRS-1 and AKT in the db/db mice were no significant changes compared with the db/m mice. However, changes were found in the phosphorylation expression of IRS-1, PI3K, and AKT. The expression of p-IRS1(S307)/IRS1 in the diabetic group was higher than that of the db/m group (p<0.01), p-PI3K(110) was lower(p<0.01), and p-AKT(S347)/AKT was lower(p<0.001). Worth to mention, treatment with ECH caused remarkable restoration of these protein expressions in contrast with the diabetic group. The expression of P-IRS1(S307)/IRS1 was decreased(p<0.05), but p-PI3K (110)(p<0.05) and p-AKT(S473)/AKT(p<0.01) were enhanced.

Discussion

In recent years, T2D-induced cognitive dysfunction is gaining attention, and some researchers refer to AD as type 3 diabetes mellitus or cerebral diabetes mellitus, which reinforces the strong link between T2D-induced cognitive dysfunction and AD[13]. Studies have shown that chronic inflammation, Aβ deposition, P-Tau and some cell signaling pathways play a very important role in the disease progression of both T2D and AD. In study, we demonstrated that ECH ameliorates T2D-induced cognitive dysfunction in db/db mice. Our study showed that ECH ameliorates the histomorphologic damage of the hippocampus and Improve cognitive and learning functions in diabetic mice[50]. Moreover, ECH reduced the mRNA and protein expression of CD44. Subsequently, our mechanistic experiments verified that ECH affected the phosphorylation of GSK-3β and Tau, as well as the IRS-1/PI3K/AKT insulin signaling pathway in diabetic mice.

Herbal medicines are increasingly valued in the treatment of diabetes, ECH, a phenylethanol glycoside, as the most biologically active component of Cistanche tubulosa, has been reported to benefit dabetic cardiomyopathy through p53/p38 MAPK and PPARα/M-CPT-1 signaling, inhibiting kidney fibrosis via TGF-β1/Smad

This article is protected by copyright. All rights reserved.
Accepted Manuscript

pathway and benefit hepatic steatosis by SREBP1c/FASN[15, 21, 51], but the role of ECH in diabetic encephalopathy has not yet been elucidated. Our study demonstrates that ECH can ameliorate hippocampal damage in diabetic encephalopathy, which may provide some new options for the treatment of patients with diabetic encephalopathy.

IRS1 is a substrate of the islet receptor tyrosine kinase that can be activated and plays an important role in insulin signaling[11]. Tyrosine phosphorylation of IRS exposes binding sites for numerous signaling chaperones to bind to, among which PI3K/Akt affects insulin function. In recent years, it has also been found that the PI3K/Akt pathway can lead to hippocampal damage, neuroinflammation, and can promote Tau phosphorylation through GSK-3β leading to cognitive dysfunction[49, 50, 52]. In our study, we found that ECH can ameliorate hippocampal damage and Tau hyperphosphorylation through the IRS1/PI3K/Akt pathway, which may provide a better understanding of the pathogenesis of diabetic encephalopathy.

CD44 is a cell surface glycoprotein that has been shown to be highly expressed in pancreatic islets and renal cortex of diabetic mice and has been shown to promote Tau accumulation, CD44 has also been shown to influence the progression of hepatocellular carcinoma and cholangiocellular carcinoma through the Akt pathway [40, 41, 53], our study found elevated brain CD44 levels in db/db mice and a significant decrease after ECH treatment.

The limitation of our study is that we did not elucidate the specific mechanism by which ECH regulates the IRS/PI3K/Akt pathway, and we did not use classical akt pathway inhibitors to compare the effect of ECH, we will continue to pay attention to this issue and perform further studies. And we

In conclusion, our identification of ECH as a drug that can ameliorate diabetic encephalopathy via CD44 and the IRS1/PI3K/Akt pathway provides a new option for the treatment of patients with diabetic encephalopathy.

Author Contributions: RH conceived and designed the experiments. JY, JZ, CY, JL, and FQ, YY, and NY performed the experiments. FQ and YY analyzed data and contributed reagents, materials, and analysis tools. FQ interpreted the results and wrote the paper. All authors made contributions to the article and approved the final version for submission.

Declarations

Ethics approval and consent to participate

The Institutional Animal Care and Use Committee(IACUC) of Renmin Hospital of Wuhan University granted approval for the experimental procedures (Issue number:WDRM20190517)

Consent for publication

Not applicable.

This article is protected by copyright. All rights reserved.

Accepted Manuscript

Available of data and materials

The GEO database was obtained from https://www.ncbi.nlm.nih.gov/geo/. The Hiplot are available from https://hiplot.com.cn/cloud-tool/drawing-tool/list). The Enrichment analysis are available from http://metascape.org/gp/index.html#/main/step1). The PPI network was obtained from https://string-db.org/.

Funding

The study was supported by the Hubei Natural Science Foundation of China. Grant No.2016CFB673.

Conflicts of Interest: The authors declare no conflict of interest.

Reference

Fig.1 (A) The Wayne diagram shows differentially expressed genes(DEGs) in the microarray datasets GSE122063 and GSE161355. (B) CD44 expression of temporal cortex in GSE122063 and GSE161355. *P<0.05, ***P < 0.001, unpaired T-test. (C) Gene Ontology (GO) enrichment bubble diagram analysis of the common DEGs between AD and T2D. (D)PPI network of relative protein in homo sapiens.

Table 1. GO enrichment analysis of the common DEGs between AD and T2D.

Fig.2 Measurements of general health conditions and insulin resistance in db/m, db/db, and db/db-ECH group. (A)Body weight gain, circle = db/m group, rectangle = db/db group, triangle = db/db-ECH group. (B) Fasting plasma glucose(FPG), circle = db/m group, rectangle = db/db group, triangle = db/db-ECH group. (C) Fasting insulin(FINS)(mIU/L), the left column = db/m group(6.56±0.19), the middle column = db/db group(22.09±0.48), the right column = db/db-ECH group(8.56±0.54). (D) Oral Glucose Tolerance Test(OGTT)(mmol/L), circle = db/m group, rectangle = db/db group, triangle = db/db-ECH group. (E) Plasma glucose area under the curve (AUC) of OGTT(*100 mmol/L*min), the left column = db/m group(12.44±0.53), the middle column = db/db group(36.93±0.53), the right column = db/db-ECH group(21.00±1.26). (F) Insulin resistance index, the left column = db/m group(0.81±0.05), the middle column = db/db group(3.21±0.06), the right column = db/db-ECH group(1.44±0.11), (HOMA-IR = FPG × FINS/22.5). Compared with db/db group, *P<0.05, **P < 0.01,*P < 0.001. Compared with db/m group, $^{\#\#\#}P$ < 0.001. n = 7 per all group.**

Fig.3 Morris water maze assessments in db/m, db/db, and db/db-ECH group.(A) Escape latency during five days of training (red = db/m group, yellow =db/db group, purple = db/db-ECH group). (B) The escape latency on day5, the left column = db/m group(20.29±3.02), the middle column = db/db group(38.73±4.52), the right column = db/db-ECH group(21.60±1.89). (C) Numbers of target platform crossings, db/m group(1.86±0.12), db/db group(0.57±0.17), db/db-ECH group(1.86±0.35). (D) mean speed in target quadrant, db/m group(13.93±0.36), db/db group(8.34±0.39), db/db-ECH group(11.79±0.47). (E) Time in target quadrant, db/m

This article is protected by copyright. All rights reserved.

Accepted Manuscript

group(31.24±1.78), db/db group(17.14±1.05), db/db-ECH group(27.12±1.96). (F) Representative swimming tracks. Mean ± SEM. n = 7 per group. *P<0.05, **P < 0.01,*P < 0.001, one-way ANOVA. Compared with db/db group, *P<0.05, **P < 0.01,***P < 0.001. Compared with db/m group, $^{\#\#}P$ < 0.01. n = 7 per all group.**

Fig.4 (A) The HE staining diagram of the hippocampus in mice from the db/m, db/db, and db/db-ECH group. DG: dentate gyrus, CA3: field CA3 of the hippocampus, CA1: field CA1 of the hippocampus (Magnification: ×200, bar = 50 μm). (B)The Nissl staining diagram of the hippocampus in mice from the db/m, db/db, and db/db-ECH group (Magnification: ×400, bar = 20 μm). (C) Quantitative analysis for the neuron number of the hippocampus by Nissle staining, the left column = db/m group, the middle column = db/db group, the right column = db/db-ECH group. Mean ± SEM. n = 7 per group. *P<0.05, **P < 0.01,*P < 0.001, one-way ANOVA.**

Fig.5 (A)CD44 mRNA expression by qRT-PCR. (B) CD44 protein expression by western blot. Mean ± SEM. *P<0.05, **P < 0.01,*P < 0.001 , one-way ANOVA.**

Fig.6 (A)The expression of GSK-3β、p-GSK-3β(Ser9)、tau and p-tau(Ser202/Thr205) in brain tissue from the db/m, db/db, and db/db-ECH group. (B)Quantitative assessment of these proteins. Mean ± SEM. *P<0.05, one-way ANOVA. (C)The expression of IRS, p-IRS(S307), P-PI3K(110), AKT, and P-AKT(S473) in brain tissue from the db/m, db/db, and db/db-ECH group. (D)Quantitative assessment of these proteins. Mean ± SEM. *P<0.05, **P<0.01, ***P<0.001, one-way ANOVA.

This article is protected by copyright. All rights reserved.

Accepted Manuscript

Table 1. GO enrichment analysis of the common DEGs between AD and T2D.

Category	Term	Description	P	Gene
Biological Processes	GO: 0006954	inflammatory response	0.009462311	SERPINA3, SPP1, CD44
	GO: 0006986	response to unfolded protein	0.020729416	DNAJB1, HSPB1
Cellular Components	GO: 0042995	cell projection	0.001755779	SPP1, CD44, GFAP
	GO: 0070062	extracellular exosome	0.003577379	DNAJB1, SERPINA3, SPP1, HSPB1, CD44
Molecular Functions	GO: 0044183	protein binding involved in protein folding	0.018695455	DNAJB1, HSPB1
	GO: 0051082	unfolded protein binding	0.047063495	DNAJB1, HSPB1
	GO: 0005178	integrin binding	0.056947804	SPP1, GFAP
	GO: 0005515	protein binding	0.059081429	DNAJB1, CD44, GEM, GFAP MAFF,SERPINA3, SPP1, HSPB1,

This article is protected by copyright. All rights reserved.

Accepted Manuscript

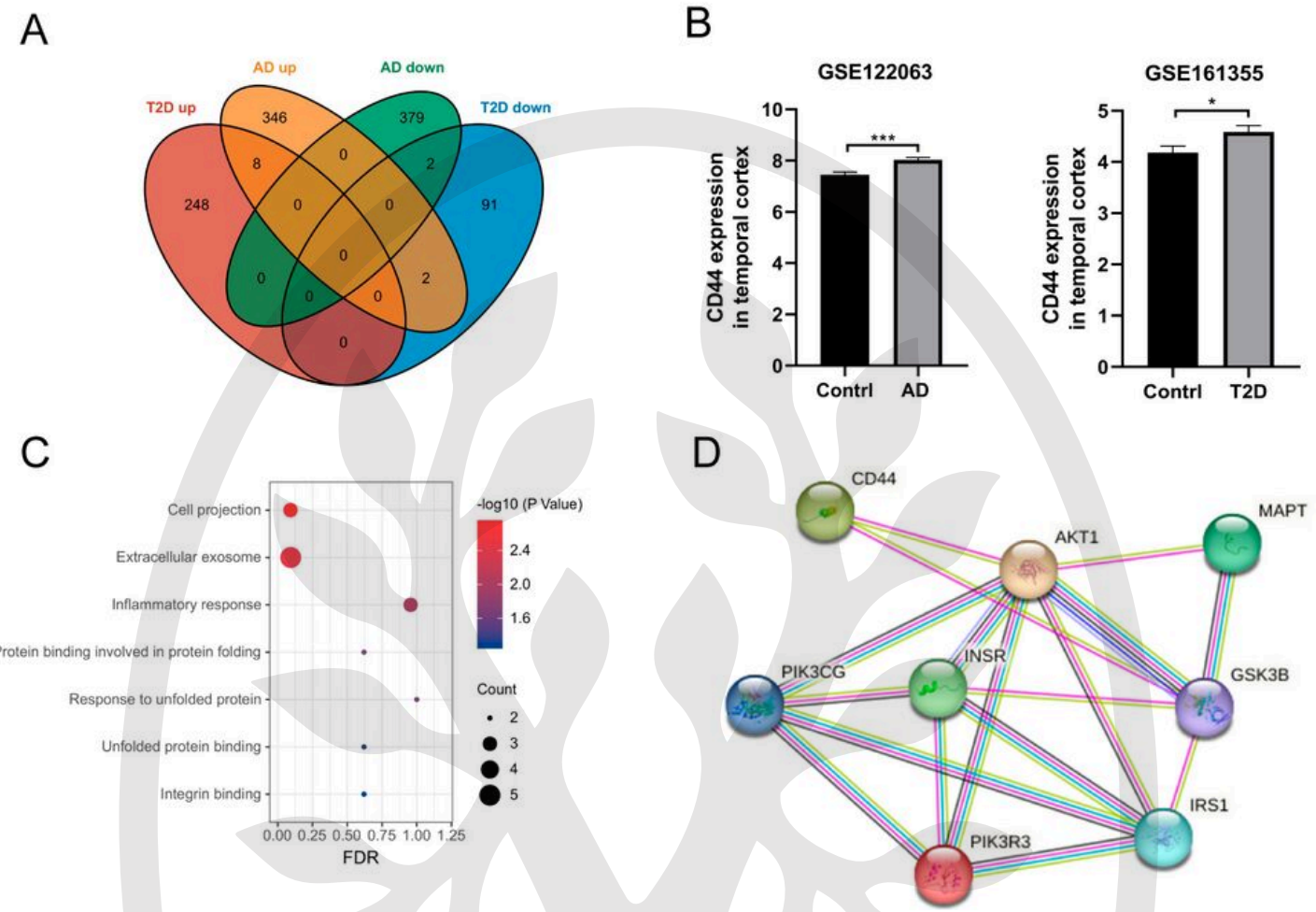

This article is protected by copyright. All rights reserved.

Accepted Manuscript

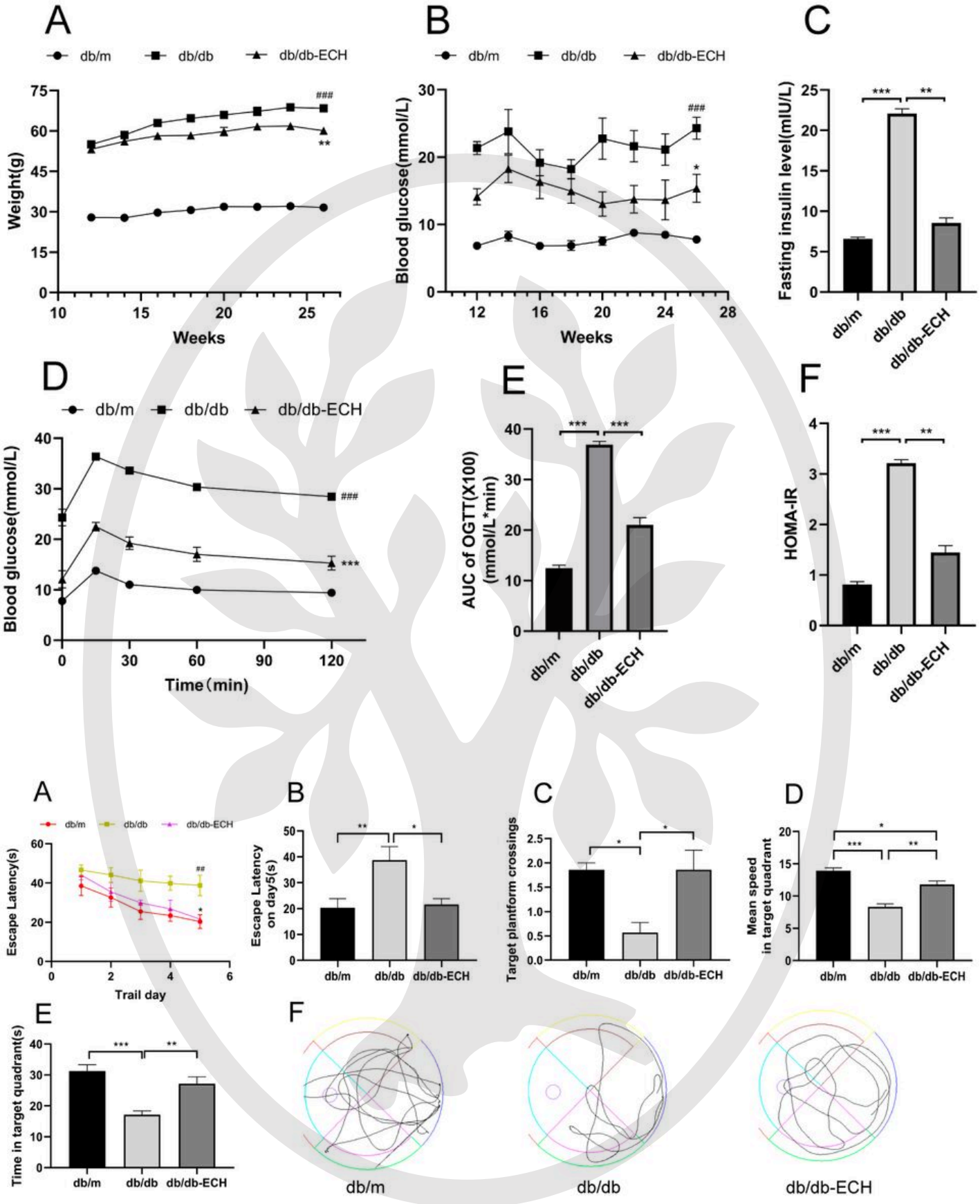

This article is protected by copyright. All rights reserved.

Accepted Manuscript

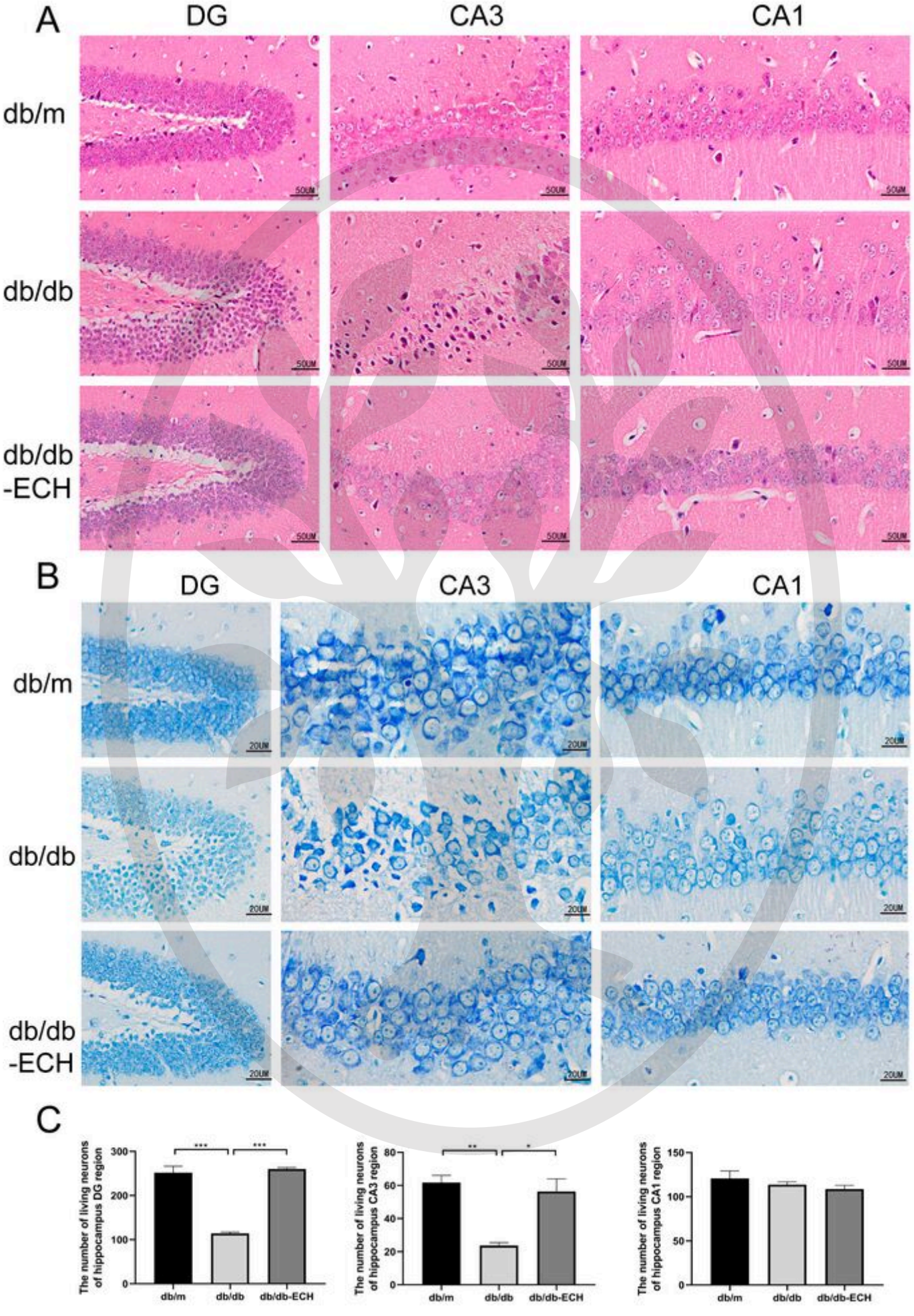

This article is protected by copyright. All rights reserved.

Accepted Manuscript

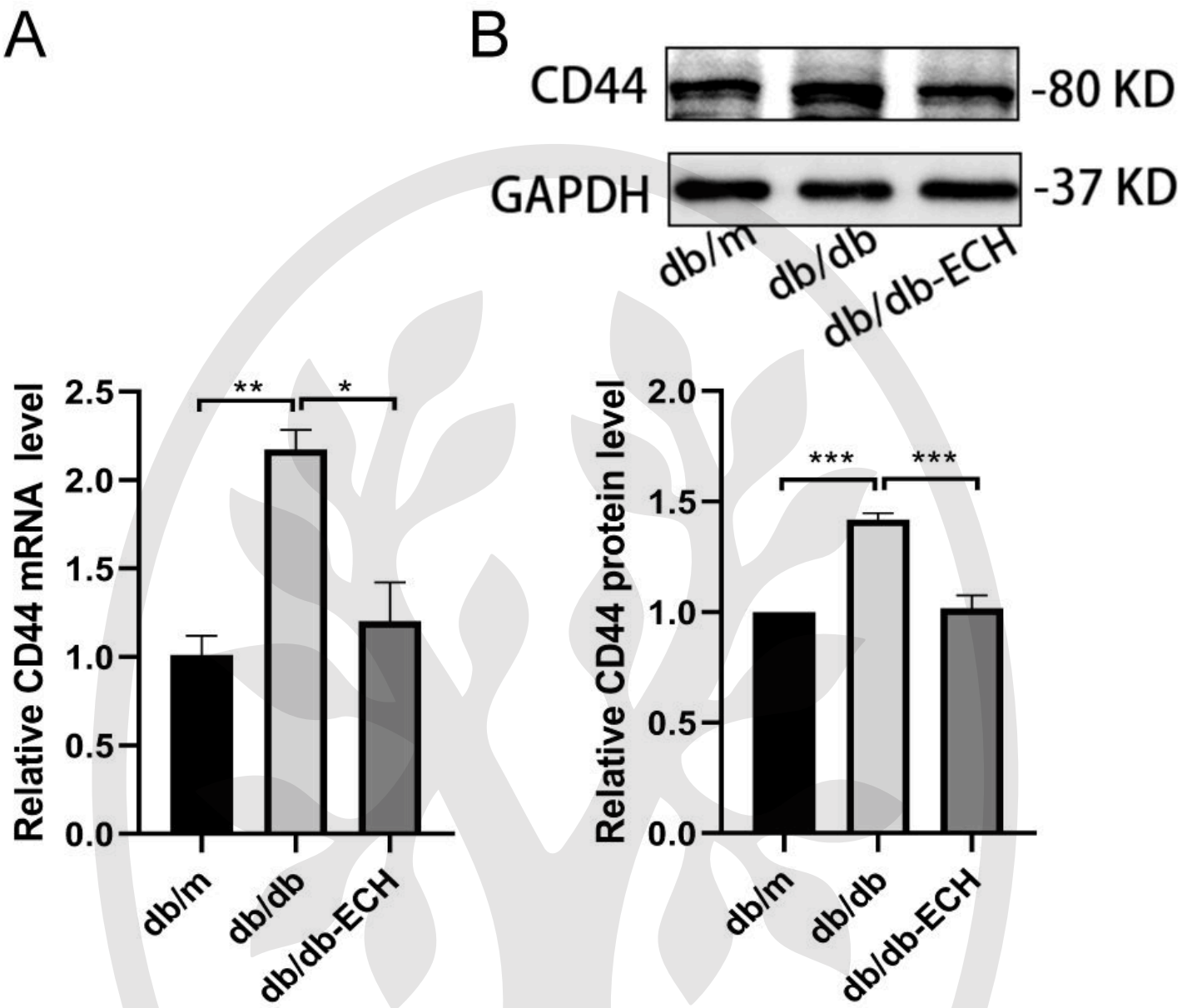

This article is protected by copyright. All rights reserved.

Accepted Manuscript

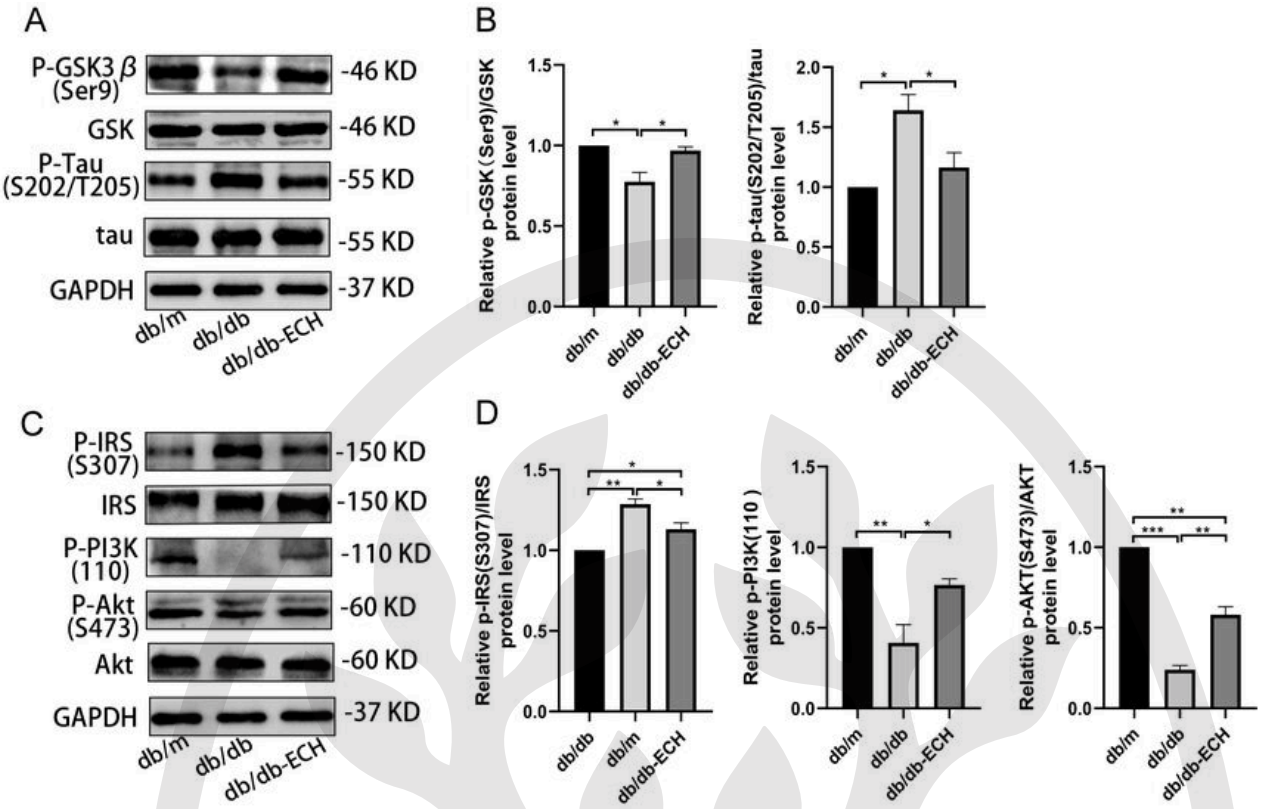

This article is protected by copyright. All rights reserved.

Accepted Manuscript